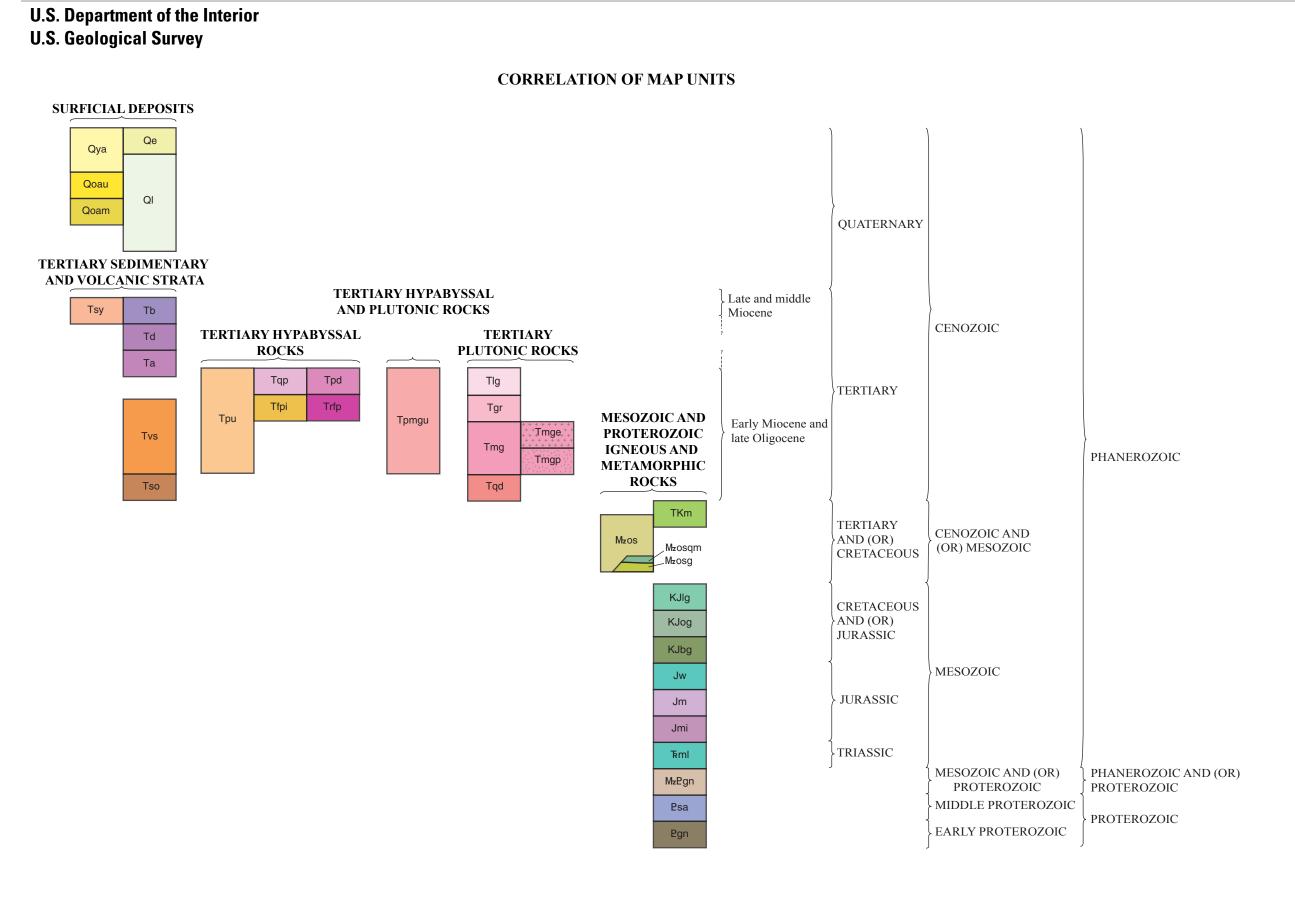
Prepared in cooperation with the Open File Report 2018-1191 U.S. Navy and U.S. Marine Corps



CALIFORNIA hade image based on 30-mete Figure 1. Index map of southeastern California showing location of Chocolate Mountain Aerial Gunnery Range.

Gulf of California

Figure 2a. Physiographic provinces of southern California in relation to faults of the San Andreas Fault System--sourced from Jahns (1954), Silver and others (1977), Powell and Silver (1979), U.S. Geolgocial Survey, Earthquake Hazards Program (2016), and Powell (1993).

DESCRIPTION OF MAP UNITS

SURFICIAL DEPOSITS Younger alluvial and debris-flow deposits (Quaternary)—Sand, gravelly sand, and sandy gravel; deposited in washes and piedmont alluvial fans Eolian deposits (Quaternary)—Windblown sand

Lacustrine deposits (Quaternary)—Mudstone and silty sandstone that contain channel deposits of sand and gravelly sand, locally fossiliferous; likely part of Brawley Formation Older alluvial and debris-flow deposits—Ouaternary. Unit includes upper and

middle subunits mapped within the gunnery range and a lower subunit that crops out along Salt Creek just north of the gunnery range boundary Older alluvial and debris-flow deposits, upper unit (Quaternary)—Sandy gravel and gravelly sand; deposited in piedmont alluvial fans. Geomorphic surface developed on deposits is typically smooth, well-developed desert pavement characterized by interlocking pebbles and dark desert varnish. Pavement underlain by pale brown, calcareous, vesicular, loessy windblown silt (pedogenic Av horizon); in turn underlain by reddened (7.5YR, Munsell colors), clayey pedogenic Bt horizon; in turn underlain by chalky, well cemented Bk horizon

Older alluvial and debris-flow deposits, middle unit (Quaternary)—Predominantly sand and pebbly sand that contains scattered cobbles; locally, contains bouldery beds; typically very thin- to thin-bedded; channel cross-bedding is common. Unit is typically very well cemented and commonly is capped by remnants of a roughly planar geomorphic surface, deeply incised, that represents an old soil stripped to the Bk horizon. In some wash walls along Salt Creek just north and outside of the Chocolate Mountain Aerial Gunnery Range, unit overlies exposures of a lower, more steeply tilted, and very well cemented unit of bouldery, sandy gravel

TERTIARY SEDIMENTARY AND VOLCANIC STRATA Sedimentary rocks younger (Tertiary)—Fluvial sandy gravel interbedded with middle and late Miocene basalt (unit Tb). Includes conglomerate of Bear Canyon of Dillon (1976). As mapped, unit may also include younger Miocene or Pliocene deposits

Basalt (Tertiary)—Flows of olivine basalt interlayered within Tertiary sedimentary rocks (unit Tsy). Five samples from basalt flows exposed in southernmost part of this study area have yielded K-Ar dates ranging from about 11 to 7 Ma, averaging 9.3±0.1 Ma (tables 2, 3). Previously published dates from basalts in Peter Kane Mountain area to the south across State Highway 78 have yielded K-Ar dates in the range of 13.4 to 9.6 Ma (Crowe and others,

Dacite (**Tertiary**)—Massive, gray, biotite microphenocrysts in siliceous matrix; resistant cliff-former; overlies and may be in part intrusive into volcanic and sedimentary rocks (unit Tvs)

1979; Needy and others, 2007)

Andesite (Tertiary)—Occurs as flows in Tabaseca Tank area in northeasternmost Chocolate Mountains **Volcanic, volcaniclastic, and sedimentary rocks (Tertiary)**—Interlayered silicic flows, tuffs, volcaniclastic rocks, and volcanic-clast conglomerate. Flows are massive to flow-banded rhyolite and (or) rhyodacite; phenocrysts consist of quartz, biotite, and feldspar in brown or pinkish-gray or maroon aphanitic matrix. Tuff beds include pyroclastic welded tuff and unwelded, white to greenish-gray, thin-bedded to massive lithic airfall tuff that contains clasts of comagmatic silicic flow rocks. Discontinuous layers of obsidian vitrophyre occur locally. Conglomerate contains clasts of volcanic rocks and, in places, crystalline-basement rocks. As mapped, may include intrusive volcanic and hypabyssal rocks. Tilted volcanic rocks in the southern Chocolate Mountains

just north of Highway 78 have yielded 40Ar-39Ar dates of 25.8±0.1 to

21.9±1.1 Ma and 17.9±2.9 Ma (tables 1, 3) edimentary rocks, older (Tertiary)—Sedimentary rocks that consist of breccia, conglomerate, sandstone, mudstone, limestone, and tuff. Clastic rocks typically are redbeds. Breccia and conglomerate beds contain clasts of Proterozoic and Mesozoic gneissic and plutonic units and contain no clasts of Orocopia Schist or Tertiary magmatic rocks. Likely correlative with the upper Oligocene to lower Miocene Diligencia Formation of Crowell (1962) in the Orocopia Mountains

TERTIARY HYPABYSSAL ROCKS Porphyry rocks, undivided (Tertiary)

Quartz porphyry—Phenocrysts of quartz and feldspar in an aphanitic felsic matrix; leucocratic. Occurs in swarm of orange-weathering dikes at north end **Pyroxene dacite**—Flow-banded dacite that contains sparse microphenocrysts

of pyroxene, hornblende, and plagioclase (andesine) Intermediate feldspar porphyry—Dacitic; white feldspar phenocrysts in aphanitic matrix; gray to dark gray or greenish gray or maroon. Intruded by dikes of quartz porphyry (unit Tqp). As mapped, unit may contain volcanic Rapakivi feldspar porphyry—Rhyodacite porphyry containing abundant

phenocrysts of plagioclase and rapakivi-textured orthoclase, typically 1 to 3 cm in diameter, and less abundant phenocrysts of hornblende, biotite, and resorbed quartz. As mapped, unit may contain volcanic rocks

TERTIARY HYPABYSSAL AND PLUTONIC ROCKS Porphyry and monzogranite, undivided (Tertiary)—Hornblende-biotite monzogranite (unit Tmg) intruded by light-colored hypabyssal porphyry (unit Tpu); underlies northwesternmost part of Chocolate Mountains TERTIARY PLUTONIC ROCKS

[Composite batholith comprising a mafic through felsic suite of plutons that intrude Orocopia Schist] **Leucogranite** (Tertiary)—Granophyric; rusty orange-brown-weathering; commonly intensely fractured and brecciated, resulting in cavernous weather-

Granite (Tertiary)—Light-colored biotite and hornblende-biotite monzogranite that has seriate texture; includes monzogranite of Mount Barrow at southeast end of range, which contains rapakivi-textured phenocrysts of orthoclase rimmed by oligoclase that range in size from 1 to 3 cm. Granite bodies at Mount Barrow and Salvation Pass have yielded biotite-hornblende K-Ar apparent ages of 24 to 21 Ma (Miller, 1974); zircons from the granite of

Mount Barrow have yielded a U-Pb age of 24±0.2 Ma (Needy and others, Monzogranite (Tertiary)—Medium-colored, gray hornblende-biotite monzogranite. In plutons in central part of Chocolate Mountains, contains equant phenocrysts of alkali feldspar that range in size from 0.25 to 1 cm, typically

0.5 cm; also contains mafic inclusions. Locally divided into: Monzogranite, equigranular—Medium- to coarse-grained, nonporphyritic. Slight primary igneous foliation observed sparsely **Ionzogranite**, **porphyritic**—Hornblende-biotite; seriate; rapakivi-textured

feldspar phenocrysts as large as 2 cm, but more typically 0.5 to 1 cm, set in fine-grained, dark-gray matrix Quartz diorite and granodiorite (Tertiary)—Dark-colored, biotite-hornblende quartz diorite, tonalite, and granodiorite; fine- to coarse-grained. Slight primary igneous foliation observed sporadically. Contains inclusions of fineto coarse-grained gabbro and diorite; as mapped, unit contains some unmapped bodies of gabbro and diorite large enough to have been mapped

MESOZOIC AND PROTEROZOIC IGNEOUS AND METAMORPHIC ROCKS Mylonite (Tertiary and (or) Cretaceous)—Mylonite, ultramylonite, and mylo-

nitic gneiss and schist

Orocopia Schist (Mesozoic)—Metamorphosed sedimentary and volcanic rocks that display prominent schistosity. Predominantly biotite-muscovite-microcline-quartz-plagioclase (albite or oligoclase) quartzofeldspathic schist and metasandstone metamorphosed from turbidite section of graywacke sandstone and mudstone. Subordinate quartzite, marble, greenschist, serpentinite, and talc-actinolite schist that typically are associated spatially with one another and occur as isoclinally folded and discontinuous layers within quartzofeldspathic schist. Distribution of this assemblage of subordinate metavolcanic and metasedimentary rock types in the map area indicates that they occur structurally high within the Orocopia Schist, near the fault boundary between Orocopia Schist and tectonically superposed Proterozoic and Mesozoic crystalline rocks. Compositional layering is likely transposed bedding. Inverted metamorphic grade ranges from albite-epidote-amphibolite to amphibolite facies. In Mammoth Wash area, contains bodies of metamorphosed hornblende diorite containing zircons that have yielded a U-Pb date of 163 Ma (Mukasa and others, 1984). Contact relation between metamorphosed diorite and quartzofeldspathic schist is equivocal (Jacobson and others,

2000). Sedimentary zircons from quartzofeldspathic schist in the Chocolate

Mountains have yielded U-Pb dates as young as Late Cretaceous (Jacobson

and others, 2000, 2011; Grove and others, 2003). Larger bodies of subordinate rock-types mapped include: Quartzite and marble (Mesozoic)—Laminated spessartite-muscovite quartzite and very thin-layered limestone marble and calc-silicate rock. Metamorphosed from protoliths of chert and siliceous limestone, respectively Greenschist (Mesozoic)—Dark greenish-gray albite-epidote-actinolite±chlorite schist. Metamorphosed from basalt protolith. Jurassic metamorphosed diorite in the Mammoth Wash area may be related petrogenetically to the metamor-

Leucogranite (Cretaceous or Jurassic)—Foliated biotite-bearing leucocratic granitic rock; aplitic, granitic, and pegmatitic; in places contains muscovite and (or) garnet

> Orthogneiss (Cretaceous or Jurassic)—Predominantly microcline-quartz-biotite-hornblende-plagioclase quartz dioritic gneiss, commonly exhibits evidence of propylitic alteration, including chlorite, epidote, and saussuritized plagioclase. Other rock types included in unit are gneissic diorite and Biotite gneiss (Cretaceous or Jurassic)—Gneissic biotite-quartz-feldspar

granodiorite and (or) monzogranite **Winterhaven Formation(?)** (**Jurassic**)—Muscovite-quartz-feldspar phyllite; light gray and likely metasedimentary and metavolcanic (see also Dillon, Porphyritic monzodiorite, granodiorite, and quartz monzonite (Juras**sic)**—Hornblende- and biotite-bearing; quartz-poor; typically porphyritic;

characterized by lavender-tinted phenocrysts of alkali feldspar. Coarse-grained porphyritic plutonic unit spans compositional range indicated in unit name Mafic intrusive suite (Jurassic)—Mafic and ultramafic intrusive rocks that include hornblende gabbro, anorthosite, hornblendite, and diorite Mount Lowe intrusive suite of Barth and Ehlig (1988) (Triassic)—Light-col-

ored monzodiorite that contains large phenocrysts of hornblende and alkali feldspar in a feldspar-rich matrix; quartz typically less than 10 percent; also contains phenocrysts of sphene and, in places, garnet. Occurs as inclusions within Tertiary hypabyssal rocks in northern part of Chocolate Mountains and is co-mingled intrusively and (or) tectonically with Mesozoic orthogneiss in the southern part; dikes and sills reported by Dillon (1976) not observed during this study Gneiss (Mesozoic and (or) Proterozoic)—Interlayered orthogneiss; light-gray,

coarse-grained, muscovitic and feldspathic quartzite; garnet-muscovite-quartz±kyanite±sillimanite pelitic gneiss; and calc-silicate gneiss. As mapped, also may include metamorphosed Paleozoic rocks Svenite, anorthosite, and anorthositic gabbro (middle Proterozoic)—Syenite consists predominantly of mesoperthite, plagioclase, minor quartz, and uralite and biotite pseudomorphous after orthopyroxene. Anorthosite and anorthositic gabbro predominantly contain andesine and uralite that is pseudomorphous after orthopyroxene. These rocks occur in northeasternmost Chocolate

Mountains in small, isolated domain that is offset sinistrally along Salt Creek Fault from larger domain in southern Orocopia Mountains **Gneiss (early Proterozoic)**—Consists of paragneiss and orthogneiss: coarse-grained sillimanite-biotite-quartz-feldspar gneiss; laminated biotite-quartz-plagioclase-alkali feldspar gneiss; amphibolite; light-colored biotite-quartz-feldspar granitic gneiss; dark-colored biotite-quartz-plagioclase-alkali feldspar augen gneiss that contains megacrysts as long as 3 cm of alkali feldspar and that originated as rapakivi-textured porphyritic granodi-

EXPLANATION OF MAP SYMBOLS Contact—Solid where location is accurate; dotted where location is concealed **Faults**—Solid where location is accurate; dotted where location is concealed;

queried where identity is questionable Normal fault—Ball and bar on downthrown block; lineation on fault surface—showing bearing and plunge Strike-slip fault—Arrows show relative motion

orite to monzogranite

Detachment fault—Boxes on upper plate Folds—Dashed where identity and existence certain, location approximate Plunging anticline—anticlinorium; axial plane trace, approximately located;

large arrowhead shows direction of plunge **Dike**—Igneous; intrusive; hypabyssal PLANAR POINT FEATURES Strike and dip of bedding

Inclined Strike and dip of primary igneous foliation Inclined Strike and dip of metamorphic foliation

SAMPLE LOCATIONS Geochronological data—sample location

GEOLOGIC SUMMARY

National Elevation Dataset (NED)

The northwest-trending Chocolate Mountains are situated along the northeastern margin of the southern Salton Trough (figs. 1, 2a). The Chocolate Mountain Aerial Gunnery Range occupies most of the 75-km-long part of the Chocolate Mountains that lies between Salt Creek to the north and California State Highway 78 to the south. Mapping studies in the Chocolate Mountains within the gunnery range are few (Dillon, 1976; Powell and others, 1994; Powell, 1995; Powell and Fleck, 2008) and this study was conducted in cooperation with the U.S. Navy (Naval Facilities Engineering Command Southwest, San Diego, California) and U.S. Marine Corps (Range Management Department, Marine Corps Air Station,

Crystalline basement rocks in the Chocolate Mountains range in age from early Proterozoic to middle Cenozoic. Early and middle Proterozoic metamorphosed sedimentary and plutonic rocks include sillimanite-biotite-quartz feldspar gneiss, layered biotite-quartz-feldspar gneiss, biotite-quartz-feldspar augen gneiss, and largely undeformed late Proterozoic anorthosite and syenite. These rock types, which crop out as dispersed domains in the Chocolate Mountains, are remnants—along with more extensive domains observed in the Eastern Transverse Ranges to the north and in the San Gabriel Mountains to the northwest—of an originally more continuous assemblage that has been dextrally displaced along strands of the San Andreas Fault System (Powell, 1981, 1993). Mesozoic rocks, including both metamorphic and plutonic rocks, are abundantly exposed

in approximately the southern third of the map area and occur as scattered pendants and structural outliers in the northern two thirds of the map area. Plutonic and metamorphosed plutonic rocks comprise four suites: (1) scattered small bodies of foliated rocks of the Mount Lowe intrusive suite of Barth and Ehlig (1988) (unit \(\mathbb{Rm} \)) that occur as inclusions within Tertiary hypabyssal rocks in the northern two thirds of the mountain range and are incorporated in Mesozoic orthogneiss in the southern third; (2) Jurassic mafic intrusive rocks (unit Jmi), predominantly hornblendite and hornblende gabbro and hornblende- and biotite-hornblende-bearing diorite; (3) coarse-grained Jurassic biotite-hornblende porphyritic plutonic rocks (unit Jm) that span a compositional range of monzodiorite, granodiorite, and quartz monzonite; and (4) Cretaceous and (or) Jurassic leucocratic granitic orthogneiss (unit KJlg) and biotite-hornblende-quartz-feldspar orthogneiss (unit KJog).

As with the Proterozoic rocks, the domains of Mount Lowe intrusive suite in the Chocolate Mountains are remnants of a much larger paleogeologic domain, a very large, zoned pluton that was disrupted by the evolving San Andreas Fault System (Silver, 1968, 1971; Ehlig, 1981; Dillon and Ehlig, 1993; Powell, 1993). The most extensive remnants of this pluton now crop out in the San Gabriel Mountains to the northwest across the San Andreas Fault and in the Little Chuckwalla Mountains to the northeast. Four other metamorphic suites that are wholly or partially Mesozoic originated, at least

in part, as supracrustal sedimentary and (or) volcanic strata. The first unit, muscovite-quartzfeldspar phyllite, crops out sparsely in the southwest corner of the map area and is likely a metamorphosed sedimentary or volcanic part of the Jurassic Winterhaven Formation (unit Jw). The second, in the southern third of the Chocolate Mountains, is biotite-quartz-feldspar gneiss (unit KJbg) that may be paragneiss spatially associated with the Cretaceous and (or) Jurassic orthogneiss suite (units KJlg and KJog). The third unit is paragneiss (unit MzPgn) that contains rare quartzite, marble, and metamorphosed conglomerate that are certainly formed from sedimentary protoliths. Finally, the Cenozoic and Mesozoic Orocopia Schist (Dillon, 1976; Haxel, 1977; Haxel and Dillon, 1978; Haxel and others, 2002) is predominantly muscovite-quartz-plagioclase quartzofeldspathic schist, likely metamorphosed turbiditic greywacke and mudstone. Subordinate rock types include chlorite-albite greenschist, quartzite, and marble representing metamorphosed basalt, chert, and limestone, respectively. In the Orocopia Mountains to the northwest of the Chocolate Mountains and in the Trigo Mountains to the east of the southeastern Chocolate Mountains, Orocopia Schist has yielded a few zircons that give Eocene dates (two in the Orocopia Mountains and four in the Trigo Mountains). These Eocene zircon dates are identified as outliers to the much larger number of zircons that yield Late Cretaceous dates in Orocopia, Chocolate, and Trigo Mountains and it has not been resolved whether these young dates represent the age of detrital zircons or record metamorphism of the Orocopia Schist (Jacobson and others, 2011; see also, Jacobson and others, 2017; Seymour and others, 2017).

Much of the northern two-thirds of the Chocolate Mountains in the map area is underlain by a composite batholith of late Oligocene and lower Miocene plutonic and hypabyssal rocks. Satellite bodies of these rocks also crop out in the southern third of the map area, including the monzogranite of Mount Barrow of Dillon (1976). Plutonic rocks in the batholith range in composition from mafic to felsic, including gabbro, diorite, quartz diorite, and granodiorite (collectively, unit Tqd), monzogranite (unit Tmg), and monzogranite and syenogranite (units Tgr and Tlg). The sequence of intrusion of the plutonic rocks progressed from mafic through felsic. Hypabyssal rocks include dacitic, rhyodacitic, and rhyolitic feldspar porphyry units (Tfpi, Trfp, and Tqp, respectively).

Cover strata in the Chocolate Mountains consists of sections of Tertiary sedimentary and volcanic strata of various ages that typically occur in isolated domains. In various combinations, mechanisms responsible for isolation of these domains include deposition in different settings, structural disruption during or subsequent to deposition, isolation by subsequent magma intrusion, and burial by younger deposits. A discontinuous edifice of Tertiary volcanic rocks crop out on both the northeastern and southwestern flanks of the Chocolate Mountains and represents the extrusive manifestation of the Tertiary composite batholith. Volcanic rocks include dacitic, rhyodacitic, and rhyolitic tuffs, welded tuffs, and silicic flows. Published ages for the rocks in this volcanic edifice in the Chocolate Mountains and to the southeast are largely late Oligocene and early Miocene (Crowe, 1978; Crowe and others, 1979; Needy and others, 2007). Our previously unpublished 40Ar/39Ar dates of 25.8±0.1 to 21.9±1.1 Ma and 17.9±2.9 Ma on tilted volcanic rocks in the southern Chocolate Mountains just north of Highway 78 (tables 1, 3) are consistent with zircon U-Pb dates of 24.1 to 23.2 Ma on similar rocks just to the southeast of the highway (Needy and others, 2007).

These volcanic rocks are, at least in part, younger than and locally overlap the oldest sedimentary rocks, which comprise scattered remnants of redbed sections that consist of sedimentary megabreccia, fluvial sandstone and conglomerate, and lacustrine mudstone. Sections of still younger Tertiary cover strata consist of andesite, dacite, and basalt flows that are interlayered with sedimentary strata. Our K-Ar dates on basalt flows interbedded with sedimentary strata in the southeastern Chocolate Mountains lie in the range of 10 to 7 Ma (tables 1, 3), again consistent with, but perhaps a bit younger than previously published K-Ar and ⁴⁰Ar/³⁹Ar dates in the range of 13 to 9 Ma (Haxel and Dillon, 1973; Dillon and Ehlig,

1993; Needy and others, 2007). Surficial deposits are predominantly Quaternary sediment deposited in piedmont alluvial and debris-flow aprons that flank the Chocolate Mountains. These apron deposits interfinger with braided-stream deposits along Salt Creek and lacustrine deposits on the floor of the Salton Trough.

Structure in the Chocolate Mountains manifests as late Oligocene to middle Miocene and possibly earlier extensional tectonism that culminated in exhumation of Orocopia Schist by tectonic denudation (Powell, 1995; Jacobson and others, 2007). In its early stages, tectonism was accompanied by sedimentation and by voluminous magma generation, which produced a batholithic-to-volcanic edifice. The principal structural feature is a complexly faulted, northwest-trending array of en echelon antiforms that runs the length of the range and continues southeast into Arizona and northwest into the Orocopia Mountains. In the anticlinorium core, Orocopia Schist is intruded by a late Oligocene composite batholith of mafic to felsic plutons. A succession of tectonic plates separated by detachment faults overlies the schist and plutons. The structurally lowest fault is ductile and juxtaposes mylonite against the schist. Three higher faults, all brittle, vertically stack plates of (1) Mesozoic orthogneiss, (2) little-deformed Triassic and Jurassic plutonic rocks, Proterozoic gneiss and anorthosite, and

Field relations and age data allow us to bracket sequential stages in the late Oligocene to middle Miocene (from about 28 to 13 Ma) magmatic-tectonic evolution of the Chocolate

dacitic to rhyolitic late Oligocene hypabyssal intrusive rocks, and (3) moderately to steeply

tilted supracrustal sedimentary and volcanic rocks.

Mountains. Our ⁴⁰Ar/³⁹Ar and K-Ar dates and published K-Ar dates (Miller, 1974) and U-Pb dates (Needy and others, 2007) indicate felsic plutonism occurred at 24 Ma, dacitic to rhyodacitic volcanism from 26 to 22 Ma and around 22 Ma and 18 Ma. These middle Tertiary strata are strongly tilted and are overlain by largely untilted sections of basalt (erupted from about 13 to 9 Ma) and conglomerate. Thus, detachment faulting in the Chocolate Mountains

The Chocolate Mountains extensional domain lies northeast of the San Andreas Fault (younger than about 6 Ma) and southwest of the early and middle Miocene Clemens Well-Fenner-San Francisquito-San Andreas strand of the San Andreas Fault System (fig. 2b). The spatial proximity of the extensional and strike-slip domains may be indicative of a genetic relation between the two (Powell, 1995)

occurred between 17 Ma and 13 Ma.

Constrained by reconstruction of an array of paleogeologic patterns comprising Proterozoic, Mesozoic, and Paleocene through lower Miocene rocks, the approximately 300 km displacement on the San Andreas Fault northwest of the Garlock Fault is distributed to the southeast on the San Andreas Fault (about 160 km displacement, from 5 or 6 Ma to present), San Gabriel fault (about 40–45 km, accumulated in intervals from 12 to 5 Ma and from 5 Ma to present), and Clemens Well-Fenner-San Francisquito-San Andreas Fault (about 100 km, between about 22-17 Ma and 13 Ma) (Powell and Weldon, 1992; Powell, 1993). The youngest rocks in southern California that have been offset about 300 km across all these parts of the San Andreas Fault are basalt flows in the Diligencia and Plush Ranch Formations, which are as young as 22 Ma based on whole-rock K-Ar dates (Frizzell and Weigand, 1993). Thus, timing of displacement on the Clemens Well-Fenner-San Francisquito-San Andreas Fault is coeval with the late Oligocene-middle Miocene evolution of the highly extended terrain in the

Lack of evidence for a large-displacement dextral fault in Arizona on-trend with the Clemens Well Fault, the appearance of the extensional domain of the Chocolate and Orocopia Mountains adjacent to the Clemens Well Fault and its southeastward projection, and the temporal coexistence of the two tectonic features are all compatible with a strain-transfer mechanism whereby dextral slip on the Clemens Well Fault is accommodated to the southeast by hyper-extension in the Orocopia-Chocolate Mountains block (Powell, 1995). This strain pattern precedes later development of the West Salton detachment that was associated with growth of the Salton Trough and that began perhaps as early as about 10 Ma (Matti and Langenheim, 2008). Unlike this later strain pattern, the extensional accommodation proposed here was not linked to opening of the Gulf of California, but rather occurred in an extensional zone between the Clemens Well Fault and a reconstructed zone of sinistral shear along the southern boundary of the Transverse Ranges and southwestern margin of the Chocolate

The post-extensional basalt and conglomerate sections are fully offset on the modern San Andreas Fault, predate growth of the Salton Trough, and span much of the interval between cessation of the Clemens Well-Fenner-San Francisquito-San Andreas Fault, at about 13 Ma, and start of the San Andreas Fault at about 5 or 6 Ma. In various reconstructions of the San Andreas system (Dillon and Ehlig, 1993; Matti and Morton, 1993; Powell, 1993), the basalt center dated in this study as ranging from 11 to 7 Ma restores to a position between the basalt field in the Peter Kane Mountain area that has been dated as ranging from 13 and 9 Ma and volcanic rocks in San Gorgonio Pass that consist of 10-Ma basalt flows and andesite breccia (Peterson, 1975) and 6-Ma basalt flows (Matti and others, 1985).

REFERENCES CITED

Barth, A.P., and Ehlig, P.L., 1988, Geochemistry and petrogenesis of the marginal zone of the Mount Lowe Intrusion, central San Gabriel Mountains, California: Contributions to Mineralogy and Petrology, v. 100, p. 192–204. Crowe, B.M., 1978, Cenozoic volcanic geology and probable age of inception of basin-range faulting in the southeasternmost Chocolate Mountains, California: Geological Society of America Bulletin, v. 89, p. 251–264.

Crowe, B.M., Crowell, J.C., and Krummenacher, D., 1979, Regional stratigraphy, K-Ar ages, and tectonic implications of Cenozoic volcanic rocks, southeastern California: American Journal of Science, v. 279, p. 186–216. Crowell, J.C., 1962, Displacement along the San Andreas fault, California: Geological Society of America Special Paper 71, 61 p.

Dillon, J.T., 1976, Geology of the Chocolate and Cargo Muchacho Mountains, southeasternmost California: Santa Barbara, University of California, Ph.D. dissertation, 405 p. Dillon, J.T., and Ehlig, P.L., 1993, Displacement on the southern San Andreas fault, in Powell, R.E., Weldon, R.J., II, and Matti, J.C., eds., The San Andreas Fault System: Displacement, palinspastic reconstruction, and geologic evolution: Geological Society of America Memoir 178, p. 199–216.

Ehlig, P.L., 1981, Origin and tectonic history of the basement terrane of the San Gabriel Mountains, central Transverse Ranges, in Ernst, W.G., ed., The geotectonic development of California; Rubey Volume 1: Englewood Cliffs, New Jersey, Prentice-Hall, p.

Frizzell, V. A., Jr., and Weigand, P. W., 1993, Whole-rock K-Ar ages and geochemical data from middle Cenozoic volcanic rocks, southern California: A test of correlations across the San Andreas fault, in Powell, R. E., Weldon, R. J., II, and Matti, J. C., eds., The San Andreas Fault System—Displacement, palinspastic reconstruction, and geologic evolution: Geological Society of America Memoir 178. Grove, M., Jacobson, C.E., Barth, A.P., and Vućić, A., 2003, Temporal and spatial trends of Late Cretaceous—early Tertiary underplating of Pelona and related schist beneath

southern California and southwestern Arizona, in Johnson, S.E., Paterson, S.R., Fletcher, J.M., Girty, G.H., Kimbrough, D.L., and Martín-Barajas, A., eds., Tectonic evolution of northwestern México and the southwestern USA: Geological Society of America Special Paper 374, p. 1–26. Haxel, G.B., 1977, The Orocopia Schist and the Chocolate Mountain Thrust, Picacho-Peter Kane mountain area, southeasternmost California: Santa Barbara, University of California, Ph.D. dissertation, 277 p.

Haxel, G.B., and Dillon, J., 1973, The San Andreas fault system in southeasternmost California, in Kovach, R.L., and Nur, A., eds., Proceedings of the Conference on Tectonic Problems of the San Andreas Fault System: Stanford University Publications in the Geological Sciences, v. 13, p. 322–333. Haxel, G.B., and Dillon, J., 1978, The Pelona-Orocopia schist and Vincent-Chocolate Mountain thrust system, southern California, in Howell, D.G., and McDougall, eds., Mesozoic paleogeography of the western United States: Los Angeles, Pacific Section, Society of Economic Paleontologists and Mineralogists, p. 453–470. Haxel, G.B., Jacobson, C.E., Richard, S.M., Tosdal, R.M., and Grubensky, M.J., 2002. The

Orocopia Schist in southwest Arizona—Early Tertiary oceanic rocks trapped or transported far inland, in Barth, A., ed., Contributions to crustal evolution of the southwestern United States: Geological Society of America Special Paper 365, p. 99–128. Jacobson, C.E., Barth, A.P., and Grove, M., 2000, Late Cretaceous protolith age and provenance of the Pelona and Orocopia schists, southern California—Implications for evolution of the Cordilleran margin: Geology, v. 28, no. 3, p. 219–222. Jacobson, C.E., Grove, M., Vućić, A., Pedrick, J.N., and Ebert, K.A., 2007, Exhumation of the Orocopia Schist and associated rocks of southeastern California—Relative roles of erosion, synsubduction tectonic denudation, and middle Cenozoic extension, in Cloos, M., Carlson, W.D., Gilbert, M.C., Liou, J.G., and Sorensen, S.S., eds., Convergent margin terranes and associated regions—A tribute to W.G. Ernst: Geological Society of America Special Paper 419, p. 1–37.

California margin inferred from provenance of trench and forearc sediments: Geological Society of America Bulletin, v. 123, no. 3/4, p. 485–506. Jacobson, C.E., Hourigan, J.K., Haxel, G.B., and Grove, M., 2017, Extreme latest Cretaceous-Paleogene low-angle subduction: Zircon ages from Orocopia Schists at Cemetery

Jacobson, C.E., Grove, M., Pedrick, J.N., Barth, A.P., Marsaglia, K.M., Gehrels, G.E., and

Nourse, J.A., 2011, Late Cretaceous—early Cenozoic tectonic evolution of the southern

Ridge, southwestern Arizona, USA: Geology, v. 45, no. 10, p. 951–954. Jahns, R.H., ed., 1954, Geology of southern California: California Division of Mines Bulletin Kuiper, K.F., Deino, A., Hilgen, F.J., Krijgsman, W., Renne, P.R., and Wijbrans, J.R., 2008,

Synchronizing rock clocks of Earth history: Science, v. 320, no. 5875, p. 500–504, https://doi:10.1126/science.1154339. Matti, J.C., and Langenheim, V.E., 2008, Does the West Salton detachment extend through San Gorgonio Pass, southern California? [abs.]: Proceedings and abstracts of the Southern California Earthquake Center Annual Meeting, v. 18, p. 140. Matti, J.C., and Morton, D.M., 1993, Paleogeographic evolution of the San Andreas fault in southern California—A reconstruction based on a new cross-fault correlation, in Powell, R.E., Weldon, R.J., II, and Matti, J.C., eds., The San Andreas Fault system—Displace-

ment, palinspastic reconstruction, and geologic evolution: Geological Society of America Memoir 178, p. 107–159. Matti, J.C., Morton, D.M., and Cox, B.F., 1985, Distribution and geologic relations of fault systems in the vicinity of the central Transverse Ranges, southern California: U.S.

Geological Survey Open-File Report 85–365, 27 p. McIntyre, G.A., Brooks C., Compston, W., and Turek, A., 1966, The statistical assessment of Rb/Sr isochrones: Journal of Geophysical Research, v. 71, p. 5459–5468, https://doi.org/10.1029/JZ071i022p05459. Miller, F.K., 1974, Comparison of granitic intrusions in the Orocopia and Pelona Schists,

southern California [abs.]: Geological Society of America, Abstracts with Programs, v. 6,

Mukasa, S.B., Dillon, J.T., and Tosdal, R.M., 1984, A Late Jurassic minimum age for the Pelona-Orocopia Schist protolith, southern California [abs.]: Geological Society of America, Abstracts with Programs, v. 16, no. 5, p. 323. Needy, S.K., Wooden, J.L., Barth, A.P., and Jacobson, C.E., 2007, Geochronology of igneous rocks in the Chocolate Mountains region as a means to interpret tectonic evolution of southeastern California [abs.]: Geological Society of America, Abstracts with Programs,

no. 3, p. 220–221.

v. 39, no. 6, p. 407. Peterson, M.S., 1975, Geology of the Coachella Fanglomerate, in Crowell, J.C., ed., San Andreas fault in southern California: California Division of Mines and Geology Special Report 118, p. 119–126. Powell, R.E., 1981, Geology of the crystalline basement complex, eastern Transverse Ranges, southern California—Constraints on regional tectonic interpretation: Pasadena, Califor-

nia Institute of Technology, Ph.D. dissertation, 441 p. Powell, R.E., 1993, Balanced palinspastic reconstruction of pre-late Cenozoic paleogeology, southern California—Geologic and kinematic constraints on evolution of the San Andreas fault system, in Powell, R.E., Weldon, R.J., II, and Matti, J.C., eds., The San Andreas Fault System—Displacement, palinspastic reconstruction, and geologic evolution: Geological Society of America Memoir 178, p. 1–106.

Powell, R.E., 1995, Extensional tectonism in the Chocolate Mountains, California, and its relation to the early evolution of the San Andreas fault system, in Leon T. Silver 70th birthday symposium and celebration: California Institute of Technology Division of Geological and Planetary Sciences, p. 91–96. Powell, R.E., and Fleck, R.J., 2008, Geology and tectonics of the Chocolate Mountains [abs.]: Proceedings and abstracts of the Southern California Earthquake Center Annual Meeting,

Powell, R.E., and Silver, L.T., 1979, Geologic analysis of ASTP photographs of parts of southern California, in El-Baz, F., and Warner, D. M., eds., Earth observations and photography: Apollo-Soyuz Test Project summary science report, v. 2: Washington, D.C., National Aeronautics and Space Administration NASA SP-412, p. 9-27. Powell, R.E., and Weldon, R.J., II, 1992, Evolution of the San Andreas fault: Annual Review of Earth and Planetary Sciences, v. 20, p. 431–468.

Powell, R.E., Hall, R., and Dawson, M., 1994, Preliminary geologic map of the Chocolate Mts. and vicinity, Salton Sea, Eagle Mts., and Trigo Mts. 30' x 60' quadrangles, southern California [abs.]: Geological Society of America, Abstracts with Programs, v. 26, no. 2, Renne, P.R., Swisher, C.C., Deino, A.L., Karner, D.B., Owens, T., and DePaolo, D.J., 1998, Intercalibration of standards, absolute ages and uncertainties in 40Ar/39Ar dating:

Chemical Geology, v. 145, p. 117–152, https://doi.org/10.1016/S0009-2541(97)00159-9. Seymour, N.M., Strickland, E.D., Singleton, J.S., and Stockli, D.F., 2017, Subduction and metamorphism of the Orocopia Schist, northern Plomosa Mountains, west-central Arizona: Insights from zircon U-Pb geochronology [abs.]: Geological Society of America, Abstracts with Programs, v. 49, no. 6. doi: 10.1130/abs/2017AM-300952 Silver, L.T., 1968, Pre-Cretaceous basement rocks and their bearing on large-scale displace-

ments in the San Andreas fault system, in Dickinson, W.R., and Grantz, A., eds. Proceedings of Conference on Geologic Problems of San Andreas Fault System: Stanford University Publications in the Geological Sciences, v. 11, p. 279–280. Silver, L.T., 1971, Problems of crystalline rocks of the Transverse Ranges [abs.]: Geological Society of America Abstracts with Programs, v. 3, no. 2, p. 193–194. Silver, L.T., Anderson, T.H., Conway, C.M., Murray, J.D., and Powell, R.E., 1977, Geologic

National Aeronautics and Space Administration NASA SP-380, p. 89-135. U.S. Geological Survey, Earthquake Hazards Program, 2016, Faults, earthquake geology, and special earthquake studies; Salton seismic imaging—Studying earthquake hazards and rifting processes in the Imperial and Coachella Valleys: U.S. Geological Survey Earthquake Hazards Program webpage, accessed July 29, 2016 and February 16, 2018, at https://earthquake.usgs.gov/research/faults/salton.php, https://earthquake.usgs.gov/static/lfs/research/SSIP InfoSheet.pdf.

features of southwestern North America, in Skylab explores the Earth: Washington, D.C.,

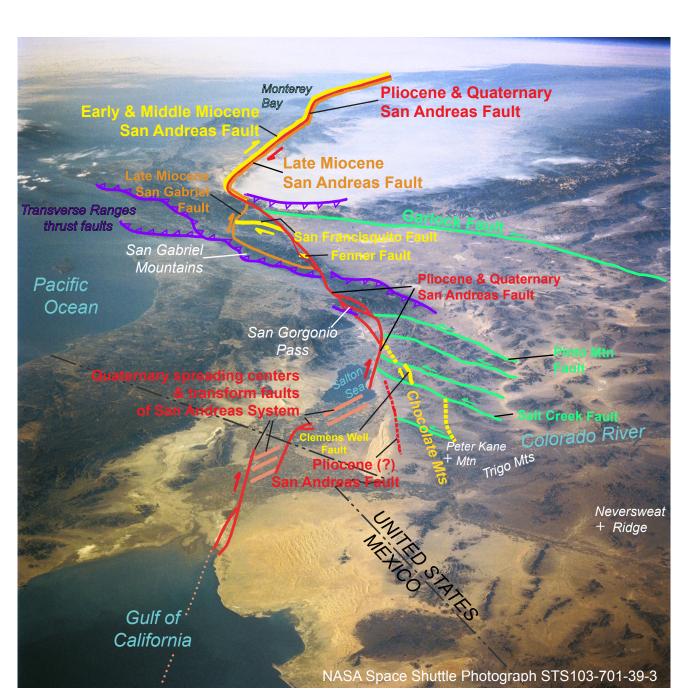


Figure 2b. Position of Chocolate Mountains in relation to selected faults of the evolving San Andreas Fault System in southern California--sourced from U.S. Geological Survey, Earthquake Hazards Program (2016), and from Powell (1993).

Table 1. Chocolate Mountains ⁴⁰Ar/³⁹Ar age data. [Volcanic-rock samples from volcanic and sedimentary section (unit Tvs). See table 3 for stratigraphic

Sample number	Mineral (method) ¹	Best estimate age (Ma) ^{2,3}	MSWD ⁴
952-19F	Plagioclase (LF)	21.87±1.09	1.70
	Plagioclase (IH)	22.95±0.13	1.05
952-19G	Biotite (LF)	23.41±0.06	1.26
	Biotite (IH)	23.42 ± 0.12	1.90
952-19G	Plagioclase (LF)	23.16± 0.15	1.83
952-20B	Plagioclase (LF)	17.9±2.9	8.87
952-20C	Plagioclase (LF)	25.17±0.19	0.29
	Plagioclase (IH)	25.79±0.13	1.40

¹Extraction method: LF, laser fusion; IH, incremental heating. ²Adjusted to Fish Canyon sanidine standard age of 28.198 Ma (Kuiper and others, 2008) ³Uncertainties shown at 1 standard error of the mean. ⁴Mean square of weighted deviates (McIntyre and others, 1966).

Table 2. Chocolate Mountains K-Ar data from basalt samples. [Basalt samples from flows (unit Tb) interbedded with sedimentary strata (unit Tsy). See table 3 for stratigraphic positions of samples

stratigraphic positions of samples					
Sample number	Age (Ma)¹	±Age(Ma)	Sample age (Ma) ²		
952-19A	8.757	0.148	8.73±0.11		
932-19A	8.692	0.162			
952-19B	9.204	0.213	9.20±0.21		
952-19C	9.224	0.203	9.22±0.20		
952-19D	9.422	0.182	9.36±0.13		
932 - 19 D	9.311	0.177			
952-19E	9 388	0.139	9 39+0 14		

Weighted mean age 9.12 ± 0.12 Ma, MSWD = 3.5

¹Ages were adjusted to GA1550 biotite standard age of 98.79 Ma (Renne and others, 1998). ²Uncertainties estimated at 1 standard error of the mean.

K-Ar dates on basalt samples from a stack of five basalt flows (unit Tb) interbedded within a little-deformed

section of sedimentary rocks (unit Tsy, here consisting of conglomerate of Bear Canyon of Dillon, 1976)

Average age for the five flows is 9.12±0.12 Ma.								
952-19D	Olivine basalt	Stratigraphically highest flow	Flow 5	9.36				
952-19C	Olivine basalt		Flow 4	9.22				
952-19B	Olivine basalt	Middle flow	Flow 3	9.20				
952-19A	Olivine basalt		Flow 2	8.73				
952-19E	Olivine basalt	Stratigraphically lowest flow	Flow 1	9.39				
⁴⁰ Ar/ ³⁹ Ar dates on volcanic samples from an older, moderately to steeply tilted volcanic and sedimentary section (unit Tvs)								
952-20C	Dacite flow	Porphyry containing phenocrysts	Apparent highest	25.8-				
		of hornblende, sanidine, and	unit in SW-	25.2				
		plagioclase	dipping section					
952-19G	Unwelded lithic	Nearly monolithologic boulder	Apparent middle	23.4-				
	tuff	breccia of unwelded biotite-	unit in SW-	23.2				
		quartz-sanidine rhyolite tuff	dipping section					
952-20B	Ignimbrite	Pyroclastic welded tuff	Apparent lowest	17.9				
			unit in SW-					
			dipping section					
952-19F	Dacite volcanic	Dacite porphyry containing	Intrusive into tuff-	23.0-				
	spine	phenocrysts of quartz,	lahar volcanic	21.9				
		hornblende, biotite,	section that					
		plagioclase, and sanidine	includes units					
			represented by					
			samples 952-19G					
			and -20B					

Geologic Map and Database of the Chocolate Mountain Aerial Gunnery Range, Riverside and Imperial Counties, California

Chocolate Mountain Aerial Gunnery Range, Riverside and Imperial Counties, California: U.S. Geological Survey Open-File Report 2018-1191, 2 sheets, scale 1: 100,000, https://doi.org/10.3133/ofr20181191.